Adsorption of atomic and molecular oxygen and desorption of silicon monoxide on Si(111) surfaces

T. Hoshino
Faculty of Pharmaceutical Sciences, Chiba University, 1-33 Yayoi-cho, Inage-ku, Chiba 263-8522, Japan
(Received 3 February 1998; revised manuscript received 31 August 1998)

Quantum chemical theoretical calculations were performed to investigate the adsorption reaction of an O_2 molecule or an O atom with a single dangling bond on the Si(111) surface and the desorption reaction of SiO gas from the O-adsorbed Si surface. The dissociative reaction of an O_2 molecule requires an activation energy of 58 kcal/mol, whereas no potential-energy barrier exists in the reaction of an O atom. The most stable O-adsorbed species has a Si-O-Si bridging configuration. This configuration is formed by a conversion from the preceding metastable species where an O atom directly attaches to a surface dangling bond. It was revealed in the SiO desorption that the dissociation of two Si-Si bonds and one Si-O bond was responsible for the SiO generation. The activation energy of each dissociation was estimated to be 89 and 44 kcal/mol, respectively. In addition, the consistency of the theoretical calculations for the kinetics of the oxygen adsorption and subsequent SiO desorption was examined under change in the size of the computational model clusters. [S0163-1829(99)10003-1]

I. INTRODUCTION

The adsorption reaction of oxygen on Si surfaces and subsequent desorption of SiO has been studied extensively[1] because of its technological importance and because of keen scientific interest. In particular, the kinetics of the O_2 reaction with a Si surface was one of the major targets in earlier studies.[2,3] Some spectroscopic observations performed at room temperatures[2] indicated that the final stable state of chemisorbed oxygen species had a Si-O-Si bridging configuration. The measurement of the surface work-function shift at very low temperatures[3] provided clear evidence for the presence of the molecular precursor preceding the final bridging configuration. These experimental findings suggested that there existed an activation energy barrier for the oxidation reaction of Si(111) surfaces with O_2 molecules. The kinetics of desorption of oxidized species on a Si surface is also an important subject in oxygen reaction with a Si surface. It is known that the monoxide SiO is produced by the sublimation of silicon oxide films at high substrate temperature and sufficiently low oxygen pressure. Pulsed molecular beam reactive scattering is a powerful technique for investigating the kinetics of those reactions.[4] Reaction of the incident O_2 or O pulses with the Si surface at substrate temperatures above ~ 1000 K leads to the production of SiO molecules. Several experiments[5,6] suggested that the reaction path of O_2 molecules on Si surfaces was via a sequential two-step process. One of these two steps was interpreted to be identical to the step detected in the reaction with an O atom. A clearer explanation, however, is required for a better understanding of the kinetics of oxidation and the etching mechanisms of Si surfaces by molecular and atomic oxygen.

Theoretical investigations of the initial stage of oxidation reaction of dimers on the Si(100)2×1 surface have already been performed by several groups.[7–10] In our previous work,[10] an oxidation reaction was examined in which an O_2 molecule was inserted into the dimer bond while keeping its molecular axis perpendicular to the surface. An activation energy of 60.4 kcal/mol was required for the dissociative reaction with the O_2 molecule. In contrast, the oxidation reaction by an O atom needs no activation energy. The activation energy estimated for the O_2 dissociative reaction is compatible with the value for one of the sequential steps obtained in the experiments by pulsed molecular-beam scattering.[5] In spite of much theoretical work,[7–10] the desorption process by SiO sublimation has not yet been fully elucidated: there remains a strong need to investigate the reaction mechanism of the desorption process of SiO on the Si surface based on a reliable theoretical approach. It is also interesting to see how the O_2 molecule or O atom interacts with a dangling bond on a Si surface. Hence, the main target of the present work is to reveal the mechanisms of the adsorption of an O_2 molecule and of an O atom on a dangling bond on the surface and the desorption of SiO species from the oxidized Si surface. In this study, first principles cluster calculations were performed to examine the process of O_2 or O reaction on the Si(111) surface at high substrate temperatures. The atomic configurations and the potential energy curves along the probable reaction paths are presented to suggest the kinetics of oxygen on Si surfaces.

II. METHOD OF CALCULATION

Two molecular models, Si_4H_9 [Fig. 1(a)] and $Si_{22}H_{21}$ [Fig. 1(b)], were used to represent the Si(111) surface structure. The small model, Si_4H_9 [Fig. 1(a)], consists of four Si atoms in the first bilayer, which provides a single surface dangling bond. This model also corresponds to the structure of a Si rest atom on the Si(111)7×7 surface. Nine H atoms were employed to terminate the outer and lower bonds for making a cluster model suitable for quantum chemical calculation. Most of the computations were performed using this small cluster with an added O_2 molecule or O atom to obtain the reaction paths and their potential-energy curves. The extended model, $Si_{22}H_{21}$ [Fig. 1(b)], contains a small

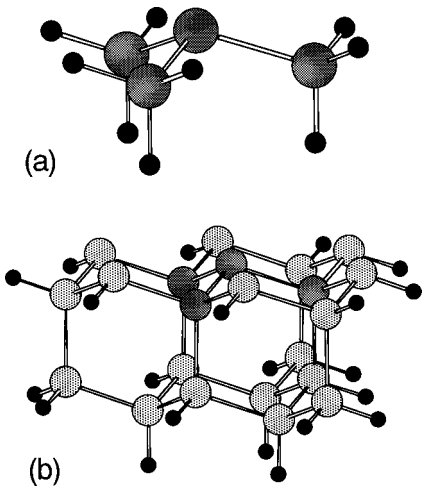

FIG. 1. Model molecules used for the cluster calculations. (a) Si_4H_9 and (b) $Si_{22}H_{21}$ clusters are employed to represent the atomic geometry of the unreconstructed Si(111) surface. Large shaded spheres denote Si atoms, where the darker spheres in (b) correspond to the four Si atoms in (a). Small solid spheres denote the hydrogen atoms used to terminate the chemical bonds at the outer and lower parts of the cluster.

cluster model (shown with hatched circles) and also includes all the second neighbor and a part of the third neighbor Si atoms from the center Si rest atom. The outer and lower chemical bonds were also embedded in H atoms. This large cluster model was employed to check the consistency of the computational results with different cluster sizes by comparing the potential-energy change during the reaction. In the initial structure, the Si-Si and Si-H bond lengths were set to 2.35 and 1.48 Å, respectively, and all bond angles were set to 109.47°. In the small cluster model, all the Si and O atoms were allowed to move independently during geometry optimization, whereas the movement of the H atoms was restricted to maintain a crystalline structure. In the large model, geometry optimization was achieved for the four inner Si atoms [darkly hatched in Fig. 1(b)] and the O atom while maintaining the initial crystalline positions for the outer Si atoms and the embedding H atoms.

The lowest potential-energy reaction paths were determined through the geometry optimization employing an *ab initio* Hartree-Fock molecular orbital (MO) method.[11] The positions of the Si and O atoms were fully optimized at any stable and saddle points with the energy gradient method.[12] It was confirmed from the vibration analysis at the optimized saddle point that a negative frequency appeared in the vibrational mode, indicating a large motion of the O atom. The intrinsic reaction coordinates (IRC) were obtained along the steepest descending gradient from the saddle point to the stable point for both directions of the reactant and product. That is, the so-called IRC calculations were carried out to confirm that the optimized saddle point was valid for the transition state of the reaction. The potential-energy change along the reaction path was estimated by total-energy calculations with the second-order Møller-Plesset perturbation theory[11] (MP-2) to include the effect of electron correlation. Because of the computational limitation, an MP-2 computation was impossible for the large cluster model. Hence, the density-functional theory (DFT) was employed for the estimation of the total energy in the computation with the large cluster. The exchange energy was computed with the gradient-corrected formula proposed by Becke,[13] and the correlation energy was with the formula derived by Lee, Yang, and Parr.[14] This method was reported to yield accurate thermochemical properties for a wide variety of molecular systems.[15] The DFT calculations were also performed with the small cluster to check the computational compatibility between the MP-2 and DFT methods. The basis set function was a standard split-valence type GTO set, 3-21G*.[16] The computer program used was GAUSSIAN94.[17]

III. RESULTS

The potential-energy changes shown in Fig. 2 represent a brief summary of the reaction of an O_2 molecule or O atom with a Si rest atom on the Si(111) surface. Paths I and II indicate the oxidation reactions by an O_2 molecule and by an O atom, respectively. Both reaction paths lead to the generation of the same reaction product on the Si surface, the ''adsorbed structure.'' This adsorbed structure is converted into a ''bridging structure'' through reaction path III. This bridging structure is the most stable species for the oxidized Si(111) surface obtained with the present model cluster. At high substrate temperatures, the SiO molecule desorbs through paths IV and V. There exists an intermediate state, the ''predesorbing state'' which is a product of path IV. An SiO molecule finally detaches from the surface through reaction path V. In the following subsections, the reaction mechanism and the potential-energy curve are presented for each reaction path in detail.

A. Oxidation by O_2 molecule (path I)

The potential-energy curve along the lowest energy path for the reaction of O_2 molecule with a dangling bond on the

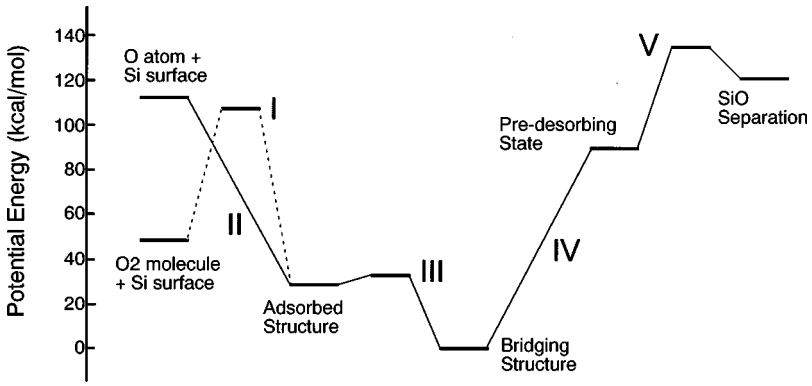

FIG. 2. Potential-energy changes during the whole process of oxidation of Si surfaces by O_2 molecule or O atom and subsequent desorption with SiO molecule. The energy is presented relative to the value for the bridging structure which is the most stable state in the reaction. The reaction process is divided into several pathways named paths I–V, connected at major stable states.

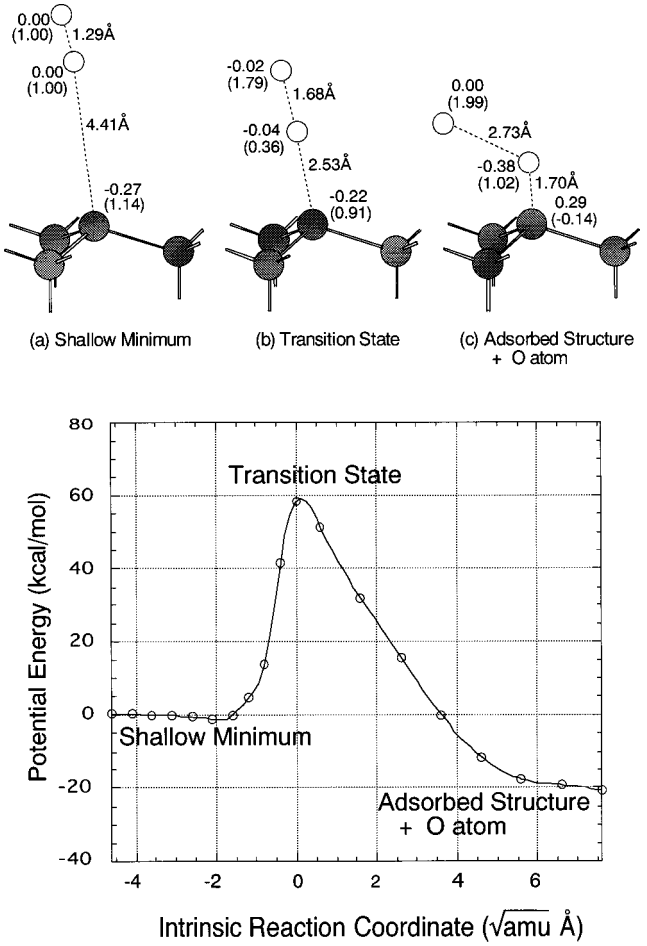

FIG. 3. Potential-energy curve along the lowest-energy reaction pathway for the oxidation by an O_2 molecule (path I in Fig. 2). The energy is presented relative to an infinite separation of the O_2 molecule from the Si surface. The abscissa represents the distance from the transition state measured in the mass-weighted Cartesian coordinates. Atomic configurations for (a) the shallow minimum, (b) the transition state, and (c) the adsorbed structure plus the O atom are exhibited with electron densities and α-spin densities (in parentheses) obtained by Mulliken population analysis. Some bond lengths are presented in units of Å , and no hydrogen atoms are shown for the sake of visual clarity. Open and shaded spheres denote O and Si atoms, respectively.

Si(111) surface is shown in Fig. 3. The zero level of this potential curve corresponds to an infinite separation of the O_2 molecule from the Si surface. Since the cluster model representing the Si surface has a single dangling bond, its electronic spin state is doublet. The electronic ground state of O_2 molecule is the spin triplet. Hence, the computation was performed with the spin quartet state for the whole system. In Fig. 3, there exists a large potential energy barrier during the reaction along path I. A shallow minimum appears before the energy barrier, which indicates a very slight stabilization compared to the initial state. The potential energy rapidly increases with an approach to the transition state. The energy at the transition state is 58 kcal/mol, which is the activation energy required for the dissociative oxidation reaction of the O_2 molecule. Beyond the transition state, the potential energy decreases steadily, and an O-adsorbed structure plus a single O atom is generated as reaction products. The stabilization energy is 21 kcal/mol.

The optimized atomic configurations and the electron populations corresponding to (a) the shallow minimum, (b) the transition state, and (c) the adsorbed structure plus the O atom are shown in the upper part of Fig. 3. In the shallow minimum, no charge transfer occurs between the Si surface and the O_2 molecule. The α-spin densities shown at the two O atoms are equal at 1.0, which indicates that the O_2 molecule keeps the initial electronic structure of the spin triplet state. In the transition state, the O_2 molecule approaches the Si surface dangling bond up to 2.5 Å, and a small amount of electrons transfers from the Si surface to the O_2 molecule. The bond length of the O_2 molecule increases to 1.68 Å from the initial value of 1.24 Å, and the α spin density begins to localize at the upper O atom, which suggests the dissociation of the O_2 molecule. In the adsorbed structure plus the O atom, the O_2 molecule is completely dissociated as confirmed by an O-O distance of 2.7 Å. The α-spin density of the separated O atom is almost 2.0, which means that this O atom is in the spin triplet state, i.e., the ground state for atomic oxygen. The Si-O bond length becomes 1.70 Å in the O-adsorbed structure, and much of the unpaired α-spin electron that was localized at the Si surface dangling bond moves to the O atom. A charge transfer of $-0.38e$ from the Si surface to the O atom also occurs.

B. Adsorption of O atom (path II)

The lowest-energy reaction path was obtained for the reaction of O atom with a dangling bond on the Si(111) surface. The potential-energy curve shown in Fig. 4 is presented relative to an infinite separation of the O atom from the Si surface. Since the electronic ground state of the final product, the O-adsorbed structure, is the spin doublet state, computations have been carried out with the spin doublet state throughout reaction path II. There exists no potential energy barrier in the adsorption reaction of the O atom. This is a prominent difference from the reaction by the O_2 molecule. The potential energy gradually decreases as an O atom approaches the Si surface, and the reaction finally results in the generation of an O-adsorbed structure. The stabilization energy of this reaction path is 84 kcal/mol compared to the initial state.

The optimized atomic configurations and the electron populations corresponding to (a) the Si surface with the O atom and (b) the adsorbed structure are also shown in Fig. 4. For the Si surface with the O atom, an unpaired β electron appears on the Si rest atom, which suggests a single dangling bond on the Si surface. The α-spin density of the O atom is 2.0, which means that the O atom is in the ground electronic state of atomic oxygen (the spin triplet state). In the adsorbed structure, a charge transfer of $-0.39e$ occurs from the Si surface to the O atom, and the α-spin density is localized on the O atom. The optimized Si-O bond length is 1.70 Å. It is important to note that the atomic configuration and the electronic structure of the adsorbed state produced by path II are identical to that obtained by path I.

C. Conversion from adsorbed structure to bridging structure (path III)

The lowest-energy reaction path for the conversion from the adsorbed structure to the bridging structure is shown in

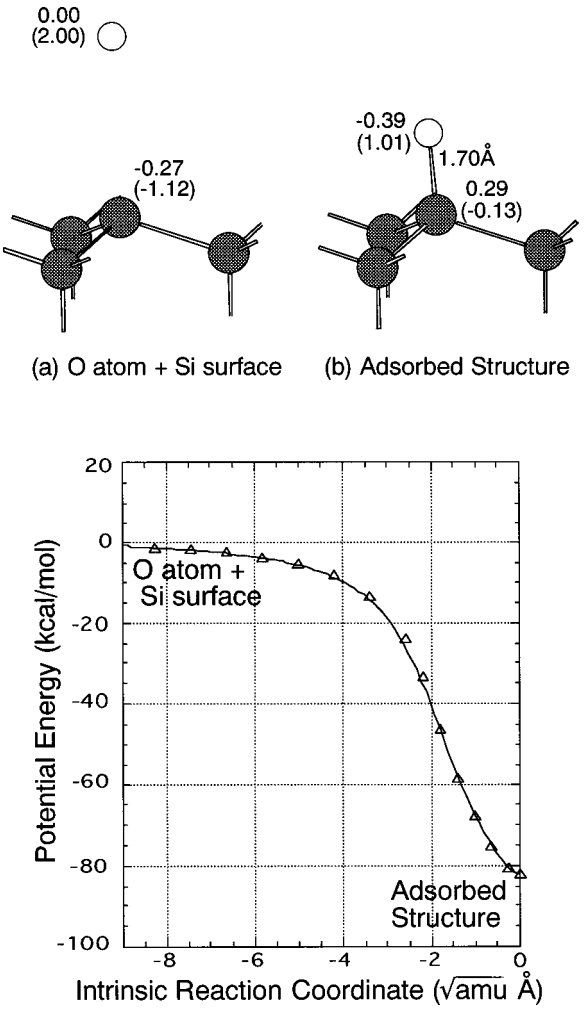

FIG. 4. Potential-energy curve along the lowest energy reaction pathway for the adsorption of O atom (path II in Fig. 2). The abscissa represents the distance measured from the adsorbed structure in the mass-weighted coordinates. Atomic configurations for (a) the Si surface with the O atom and (b) the adsorbed structure are exhibited with electron densities and α spin densities (in parentheses). See also the legend of Fig. 3.

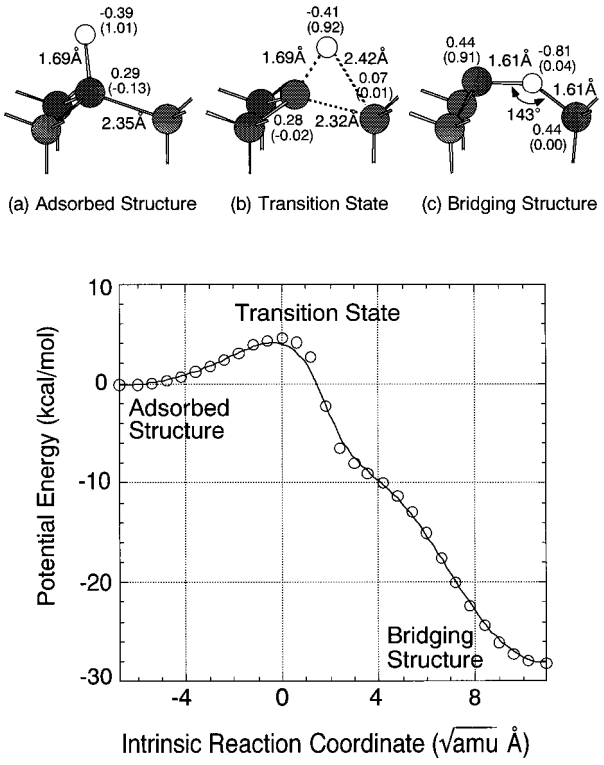

FIG. 5. Potential-energy curve along the lowest-energy reaction pathway for the conversion of the silicon oxide structure (path III in Fig. 2). The energy is presented relative to the adsorbed structure. The abscissa represents the distance from the transition state measured in the mass-weighted coordinates. Atomic configurations for (a) the adsorbed structure, (b) the transition state, and (c) the bridging structure are exhibited with electron densities and α-spin densities (in parentheses). See also the legend of Fig. 3.

Fig. 5. The potential-energy curve is presented in relative value to the adsorbed structure. Computations were performed with the spin doublet state. There appears a small potential-energy barrier for the conversion reaction of this path. The potential energy slowly increases with approach to the transition state from the adsorbed structure. The energy at the transition state is 4.4 kcal/mol; that is, the activation energy required for this conversion is trivial. Passing over the transition state, the potential energy gradually decreases, and a bridging structure is produced as a consequence of the conversion reaction. The stabilization energy is 28 kcal/mol relative to the initial adsorbed structure. The final bridging structure is the most stable among all of the states investigated in this report.

The optimized atomic configurations and the electron populations in (a) the adsorbed structure, (b) the transition state, and (c) the bridging structure are shown in the upper part of Fig. 5. The adsorbed structure is identical to the final product of paths I and II. A charge transfer occurs from the Si surface to the O atom, and much of the α-spin density concentrates on the O atom. In the transition state, the O atom leans toward one of the Si atoms in the second layer, which leads to the formation of a three member ring of O-Si-Si. The amount of the electron transfer from the Si surface to the O atom increases compared to the initial adsorbed structure, and most of the α spin density is still localized on the O atom. In the bridging structure, the O atom is completely inserted into the Si-Si bond. The two Si-O bonds assume the same length, 1.61 Å, and the Si-O-Si bond angle becomes 143°. These values are fairly close to those of crystalline SiO_2 (α-quartz[18]). The charge transfer from the Si to the O atom drastically increases to $-0.81e$. An unpaired α-spin electron transfers to the Si rest atom; that is, most of the α-spin density is localized at the Si rest atom, which indicates the presence of a single dangling bond on the rest atom. It is reasonable to conclude that the bridging structure is the typical configuration of silicon oxide on an Si(111) surface.

D. Dissociation of Si-Si bonds for SiO sublimation (path IV)

The potential-energy curve along the lowest energy reaction path for the dissociation of Si-Si bonds during the SiO desorption is shown in Fig. 6. The potential energy along this path is presented relative to the bridging structure. The reaction path was determined with the spin doublet state, but the potential energy changes were computed for both the spin doublet and the quartet states. In the spin doublet state, the

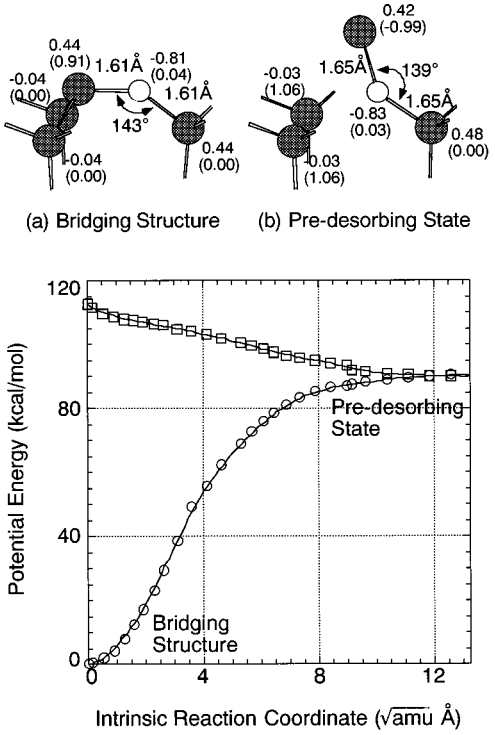

FIG. 6. Potential-energy curve along the lowest-energy reaction pathway for the dissociation of Si-Si bonds for SiO desorption (path IV in Fig. 2). The circle and square plots are for the spin doublet and quartet states, respectively. The energy and the distance in abscissa are measured from the bridging structure. Atomic configurations for (a) the bridging structure and (b) the predesorbing state are exhibited with electron densities and α-spin densities (in parentheses). See also the legend of Fig. 3.

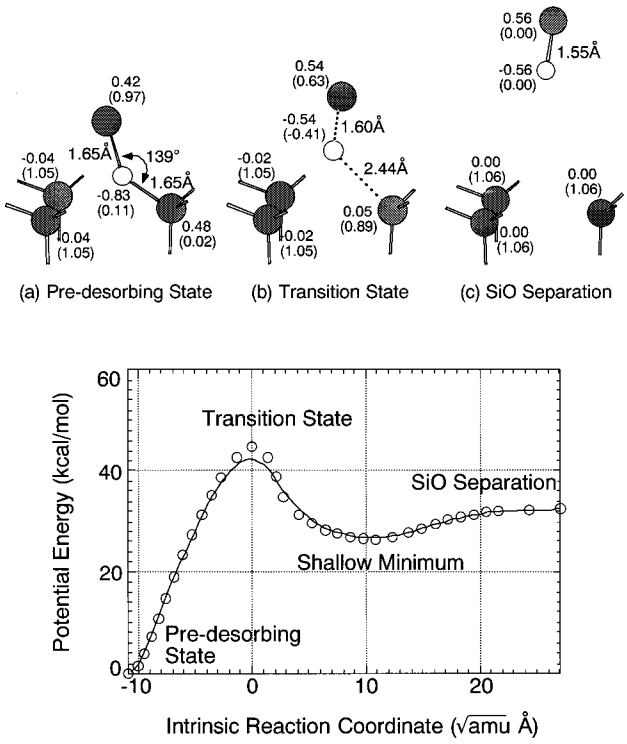

FIG. 7. Potential-energy curve along the lowest-energy reaction pathway for the detachment of the SiO molecule (path V in Fig. 2). The energy is presented relative to the predesorbing state. The abscissa represents the distance measured from the transition state. Atomic configurations for (a) the predesorbing state, (b) the transition state, and (c) the SiO separation state are exhibited with electron densities and α-spin densities (in parentheses). See also the legend of Fig. 3.

potential energy monotonically increases as the reaction progresses from the bridging structure to the predesorbing state. The energy difference between the bridging structure and the predesorbing state is 89 kcal/mol, which poses a significantly large activation energy barrier in the desorption process. In the spin quartet state, the potential energy gradually decreases from the bridging structure to the predesorbing state. In fact, the predesorbing state is located at the potential-energy minimum in the spin quartet state. This fact was confirmed by the geometry optimization with the spin quartet state. Note that the two spin electronic states, the doublet and quartet, converge to the same energy in the predesorbing state.

The optimized atomic configurations and the electron populations in (a) the bridging structure and (b) the predesorbing state are also shown in Fig. 6. The bridging structure is identical to the product of path III, where the Si-O bond lengths and Si-O-Si bond angle are close to the values of crystalline SiO_2. In the predesorbing state, the Si rest atom moves upward, and the Si-Si bonds between the rest atom and the second layer atoms are completely dissociated. The Si-O-Si bond bends to the opposite direction compared to the bridging structure. Both Si-O bond lengths are 1.65 Å, and the Si-O-Si bond angle is 139°. The electron population shown in Fig. 6(b) is the value obtained in the spin doublet state. A charge transfer of $-0.83e$ is still achieved due to the electron attraction of the O atom from the adjacent Si atoms. No significant charge transfer, however, occurs around the dissociated Si atoms in the second layer. A large density of β-spin electrons appears at the Si rest atom, and in contrast, two dissociated Si atoms in the second layer have large α-spin densities, which means that each of those Si atoms has a single dangling bond. In the predesorbing structure, the electron populations of the spin quartet state are almost the same as those of the doublet state, except that the β-spin density at the Si rest atom is substituted by an α-spin.

E. Detachment of SiO molecule (path V)

The lowest-energy reaction path for the detachment of a SiO molecule from a Si surface is shown in Fig. 7. The potential-energy curve is presented relative to the predesorbing state. Computations were performed with the spin quartet state. There exists a potential-energy barrier for the separation of the SiO molecule. The potential energy steadily increases with approach to the transition state, and the value at the transition state is 44 kcal/mol compared to the predesorbing state. Beyond the transition state, the potential energy gradually decreases, and a shallow minimum appears before the complete separation of the SiO molecule. The energy of this shallow minimum is higher than that of the predesorbing state by 26 kcal/mol. At the SiO separation, the potential energy becomes 32 kcal/mol. Therefore, the final SiO disconnection from the Si surface is required to overcome a slight energy barrier of 6 kcal/mol.

TABLE I. Comparison of potential-energy changes between the small and large cluster models. The energy differences are presented relative to the bridging structure.

	Si_4H_9+O		$Si_{22}H_{21}+O$
	MP-2 (eV)	DFT (eV)	DFT (eV)
Adsorbed structure	1.22	0.95	0.96
Bridging structure	0.00	0.00	0.00
Predesorbing state	3.88	3.67	3.66
SiO separation state	5.30	5.76	5.46

The optimized atomic configurations and the electron populations (a) in the predesorbing state, (b) in the transition state, and (c) at the SiO separation are shown in the upper part of Fig. 7. The predesorbing state is identical to the final state of path IV. The α-spin densities are localized at the two dissociated Si atoms in the second layer and the top Si atom that used to be the rest atom. In the transition state, the Si-O bond length between the O atom and the Si rest atom reduces to 1.60 Å. In contrast, the bond length between the O atom and the Si atom in the second layer expands to 2.44 Å. This structural change suggests that the dissociation of one of the Si-O bonds is responsible for the potential-energy barrier in the transition state. The charge transfer to the O atom reduces to $-0.54e$ compared to the predesorbing state with most of the charge transfer from the top Si atom. The α-spin density of the Si atom in the second layer increases, and at the same time, the spin density of the top Si atom decreases. At the SiO separation, the bond length of the SiO molecule becomes 1.55 Å. A charge transfer of $-0.56e$ occurs only in the SiO molecule. No charge transfer occurs from the Si surface to the SiO molecule. The α-spin density suggests that SiO molecule is the spin singlet state. Each of three Si atoms left on the surface after SiO desorption has an α-spin density of ~ 1.0, which suggests the presence of single dangling bond on each Si atom.

F. Comparison of computational results with small and large clusters

In order to check the dependence of the computational results on the size of the model cluster, calculations were performed with the large cluster shown in Fig. 1(b). The potential energies were obtained for the four stable states: (a) the adsorbed structure, (b) the bridging structure, (c) the predesorbing state, and (d) the SiO separation state. The geometry of every stable state was optimized with the large model. However, the DFT was employed because of the shortage of computational memory for the MP-2 level calculation with the large cluster. Furthermore, calculations with the DFT method were also carried out for the small cluster with geometry optimization for the purpose of evaluating the computational errors caused by the differences between the employed theories.

A comparison of the potential energies between small, Si_4H_9+O, and large, $Si_{22}H_{21}+O$, cluster models is presented in Table I. The potential energy is relative value with respect to the respective cluster. The bridging structure is, of course, the most stable state in every calculation. It can be seen from the small cluster calculation that some degree of error exists between the MP-2 and DFT methods. However, the potential-energy changes during the reaction generally agree with each other. Good consistency of the potential energies between the small and large models is obtained with the DFT method, except for an error in the SiO separation. From this consistency, it is safe to assume that the small cluster gives reasonable results for the potential-energy changes in the reactions addressed in this work. The structural transformation during the reaction computed with the large cluster is shown in Fig. 8. Every optimized atomic configuration of the (a) adsorbed structure, (b) bridging structure, (c) predesorbing state, and (d) SiO separation state completely agrees with those obtained by the small cluster. This agreement also supports the consistency of calculations between the small and large cluster models.

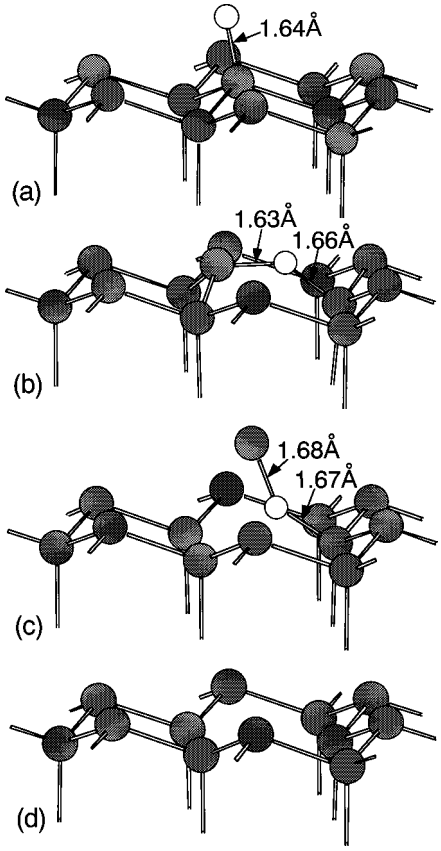

FIG. 8. Atomic configurations for (a) the adsorbed structure, (b) the bridging structure, (c) the predesorbing state, and (d) the SiO separation state, optimized with the large cluster of $Si_{22}H_{21}$ [Fig. 1(b)]. Open and shaded spheres denote O and Si atoms, respectively. Consistency is achieved with the optimized structures of the small cluster model.

IV. DISCUSSION

The theoretical calculations executed in this work have provided the following findings on the kinetics of oxidation of Si(111) surfaces and subsequent desorption of SiO. (1) The most significant difference between oxidation reactions by O_2 molecules and O atoms is in the activation energy necessary for the reactions. The dissociative oxidation reaction by an O_2 molecule requires a large activation energy of 58 kcal/mol (2.5 eV), whereas no activation energy is re-

quired for the oxidation reaction by an O atom. It is interesting to note that the activation energy estimated for the O_2 molecular reaction is very close to the value previously obtained for the oxidation of Si dimers on Si(100) surfaces:[10] namely, the dissociative reaction by an O_2 molecule requires a similar activation energy whether it attacks a Si dangling bond or a Si-Si covalent bond. (2) The silicon oxide produced by the dissociative reaction by an O_2 molecule is identical to that produced by the adsorption reaction by an O atom. Therefore, the subsequent reaction process after the adsorbed structure is common both in the reaction by an O_2 molecule and an O atom. (3) In both the oxidation reaction by the O_2 molecule and the O atom, the oxygen initially attacks a surface dangling bond and results in attachment to the Si rest atom. Subsequently, the adsorbed structure converts to the bridging structure with an oxygen insertion into the Si-Si bond. (4) In the desorption process of SiO molecule, the dissociation of the Si-Si and/or Si-O bond requires a large activation energy. An activation energy of 89 kcal/mol (3.9 eV) is required for the dissociation of two Si-Si bonds from the stable bridging structure. The subsequent detachment of the SiO molecule involves a dissociation of one Si-O bond, which requires an activation energy of 44 kcal/mol (1.9 eV). Therefore, the rate determining step for SiO desorption is concluded to be the breakage of the Si-Si network, instead of SiO detachment.

Experimental findings for the kinetics of SiO sublimation through the reaction of an O_2 molecule or an O atom with a Si surface were already provided by the pulsed-modulated molecular beam scattering studies.[5,6] Those studies suggested that the reaction of an O_2 molecule on the Si(100) surface occurred via a two-step process: $O_2(g) \rightarrow I_1 \Rightarrow I_2 \Rightarrow SiO(g)$. The reaction process involved two intermediates that were produced sequentially. In contrast, the reaction of an O atom on the Si(100) surface was suggested to follow a single step process, which involved a single intermediate: $O_2(g) \rightarrow I' \Rightarrow SiO(g)$. The rate constant in the reaction kinetics for the O atom was found to be equal to that obtained for one of the steps in the O_2 molecular reaction. Consequently, Engstrom and co-workers[5] interpreted that the intermediate I_2 was identical to the intermediate I' and the desorption kinetics of $I_2 \Rightarrow SiO(g)$ was equivalent to $I' \Rightarrow SiO(g)$, whose activation energy was estimated to be 79 kcal/mol (3.4 eV). The activation energy for the reaction path of $I_1 \Rightarrow I_2$ was reported to be 60 kcal/mol (2.6 eV). The kinetics of the reaction of an O_2 molecule with Si(111) surfaces was also reported using the pulsed-modulated molecular-beam technique.[19] The same sequential two-step process was observed for the reaction on Si(111) surfaces as well. No significant difference was found between the Si(100) and (111) surfaces in regard to the reaction rate constants. Another important finding for the kinetics of the thermal desorption of SiO on the Si(100) surface was presented by Sun, Bonser, and Engel[20] using the temperature-programmed desorption (TPD) technique. The experimental results showed that the activation energy to produce $SiO(g)$ was 85 ± 4 kcal/mol (~ 3.7 eV). The activation process was suggested to be closely involved in the decomposition of oxide films.[20,21] Judging from a comparison of the present computational results with the above data, it is plausible to interpret the experimental results as follows. (1) The activation energy of 2.6 eV, which was detected only in the reaction by O_2 molecule, is involved in the dissociation reaction of O_2 molecule. (2) The activation energy of 3.4–3.7 eV, which was measured in the SiO desorption, originates to the breakage of the bond network preceding SiO detachment. (3) The intermediate species observed as I_2 and I' is the bridging structure, where an oxygen is located between two Si atoms.

Since the initial Si surface employed in the present work has a perfect bilayer structure, a large activation energy barrier is expected for the breakage of the network of Si-Si bonds in the SiO desorption process. Once the reaction starts and the surface structure becomes disordered, the Si-Si network dissociates more easily. The structure shown in Fig. 7(c) becomes the next target for oxidation reaction by the O_2 molecule and the O atom. Therefore, the activation energy measured in experiments is a mixture of those of many reactions involving the various initial surface structures. Consequently, it would be reasonable to think that the computational value of the activation energy for the SiO desorption reported here gives an upper bound relative to the experimental data.

In this work, the reaction pathways and their potential energy changes have been clarified through the process of O_2 or O adsorption and the subsequent SiO desorption on Si surfaces. Such a reaction process has been studied by the pulsed molecular-beam scattering technique. Yu and Eldridge[6] performed the experiment with three different substrate temperatures, 850°, 900°, and 950° C. In the experiment by Engstrom and co-workers,[5] the reaction was analyzed in the temperature range of 730–900 °C. Although the clean Si(111) surface usually shows a 7×7 reconstructed structure at room temperatures, the surface barely maintains the 7×7 structure at the high substrate temperatures used in the above experiments. The critical temperature (T_c) for the 7×7 phase transition was reported to be about 830 °C,[22] and at higher temperatures than T_c, the surface structure becomes disordered and is observed as the 1×1 structure in the diffraction method. This disordered 1×1 phase can be observed with a scanning tunneling microscope (STM) even at around 500 °C when the surface is supercooled from a high temperature above T_c.[23] The motion of atoms in the 1×1 phase was reported to be very active.[24] Therefore, it is natural to assume that the detailed geometry of the surface atoms scarcely contributes to the rate-determining steps under the experimental conditions with which the desorption of SiO occurs from Si surface. In fact, the pulsed molecular beam analysis by Ohkubo *et al.*[19] showed no difference for the reaction kinetics between the Si(100) and Si(111) surfaces. This means that differences of surface atomic geometry does not dominate the reaction any more at the high temperatures. The present computations were performed with the cluster model representing the 1×1 structure of the Si(111) surface, and focused on the interaction of an O_2 molecule or an O atom with a single dangling bond on the surface. Hence, the present theoretical approach would correspond to the experimental situation in which the oxidation and subsequent desorption rapidly occurs at high temperatures. On the other hand, the present approach seems to be inadequate for the interpretation of the experimental findings obtained at room or low temperatures.[2,3] For instance, the

presence of a stable O_2 molecular precursor is difficult to account for with the present computational results. The stabilization energy at the shallow minimum in path I is too slight to be detected in experiments. And, the charge transfer between the O_2 and the Si surface hardly occurs at the shallow minimum in spite of the experimental detection of a large amount of electron transfer in the O_2 precursor state.[25] This discrepancy would intimate the possibility that the interaction of an O_2 molecule with the 7×7 structure induces another reaction process not initiated on the 1×1 surface. Accordingly, it would be significant to theoretically investigate the reaction of O_2 molecule at room or low temperatures by constructing a model cluster representing the 7×7 reconstructed surface.

In the reaction pathway examined here, the dissociative reaction of an O_2 molecule on the Si surface requires a fairly large activation energy, 2.5 eV, which suggests the difficulty of O_2 dissociation at room temperatures. In fact, an isolated O_2 molecule needs an energy of 5.1 eV to dissociate into atomic oxygen by itself.[26] Hence, the interaction with a single Si dangling bond is concluded to promote the reactivity of O_2 molecule because the activation energy is reduced by half. This finding means that the O_2 dissociative reaction requires an interaction with Si substrate. Without such interaction, O_2 molecules would hardly have a chance to initiate the oxidation. According to the estimation by Hattori,[27] only one of the 10^9 incident O_2 molecules could contribute to the oxidation on the H-terminated Si(111) surface. From this viewpoint, it would be interesting to examine the dissociative reaction of an O_2 molecule when it interacts with two dangling bonds simultaneously with a highly restricted incident posture. Such a situation would be more important in reactions at low temperatures because the total reaction rate could be occasionally dominated by a narrow reaction channel.[8,28] Accordingly, theoretical investigation of the reaction of an O_2 molecule with the 7×7 Si surface would also be important.

V. SUMMARY

Ab initio quantum chemical calculations were performed to investigate the oxidation mechanism by O_2 molecules or O atoms on Si(111) surfaces and the subsequent desorption mechanism of SiO molecules. The lowest-energy reaction paths were obtained for the whole process of the oxidation and desorption. The interaction of an O_2 molecule with the Si(111) surface leads to a dissociative oxidation which requires a large activation energy: 58 kcal/mol. In contrast, no activation energy barrier exists in the reaction of an O atom. Both the oxidation by the O_2 molecule and the O atom result in the generation of the same silicon oxidized species, where the O atom attaches on a surface dangling bond of the Si rest atom. This structure converts into a more stable structure via an activation process of 4 kcal/mol, where an Si-O-Si bridging structure is produced. In the pathway of the sublimation of an SiO molecule from the oxidized silicon surface, there appear two activation energy barriers that involve the dissociation of Si-Si and Si-O bonds. The breakage of Si-Si network requires a large activation energy, 89 kcal/mol, and the detachment of the SiO with the dissociation of the Si-O bond has another activation process of 44 kcal/mol. The SiO desorption is endothermic by 121 kcal/mol (5.2 eV) compared to the Si-O-Si bridging structure. The potential-energy changes during the reaction process have been confirmed to be consistent under the extension of the cluster model size.

ACKNOWLEDGMENTS

A part of this work was supported by a Grant-in-Aid from the Ministry of Education, Science and Culture, Japan. This work was also supported by a grant from the Futaba Electronics Memorial Foundation.

[1] T. Engel, Surf. Sci. Rep. **18**, 91 (1993).
[2] U. Höfer, P. Morgen, W. Wurth, and E. Umbach, Phys. Rev. B **40**, 1130 (1989); **39**, 3720 (1989), and references therein.
[3] C. Silvestre and M. Shayegan, Phys. Rev. B **37**, 10 432 (1988); C. Silvestre, J. Hladky, and M. Shayegan, J. Vac. Sci. Technol. A **8**, 2743 (1990).
[4] M. P. D'Evelyn, M. M. Nelson, and T. Engel, Surf. Sci. **186**, 75 (1987).
[5] J. R. Engstrom and T. Engel, Phys. Rev. B **41**, 1038 (1990); J. R. Engstrom, M. M. Nelson, and T. Engel, J. Vac. Sci. Technol. A **7**, 1837 (1989).
[6] M. L. Yu and B. N. Eldridge, Phys. Rev. Lett. **58**, 1691 (1987).
[7] Y. Miyamoto and A. Oshiyama, Phys. Rev. B **41**, 12 680 (1990).
[8] K. Kato, T. Uda, and K. Terakura, Phys. Rev. Lett. **80**, 2000 (1998).
[9] T. Hoshino, M. Tsuda, S. Oikawa, and I. Ohdomari, Surf. Sci. Lett. **291**, L763 (1993).
[10] T. Hoshino, M. Tsuda, S. Oikawa, and I. Ohdomari, Phys. Rev. B **50**, 14 999 (1994).
[11] See, for example, A. Szabo and N. S. Ostlund, *Modern Quantum Chemistry* (MacMillan, London, 1982).
[12] H. B. Schlegel, J. Comput. Chem. **3**, 214 (1982).
[13] A. D. Becke, Phys. Rev. A **38**, 3098 (1988); J. Chem. Phys. **98**, 5648 (1993).
[14] C. Lee, W. Yang, and R. G. Parr, Phys. Rev. B **37**, 785 (1988).
[15] For exapmle, K. Raghavachari, B. B. Stefanov, and L. A. Curtiss, Mol. Phys. **91**, 555 (1997).
[16] M. S. Gordon, J. S. Binkley, J. A. Pople, W. J. Pietro, and W. J. Hehre, J. Am. Chem. Soc. **104**, 2797 (1982).
[17] M. J. Frisch, G. W. Trucks, H. B. Schlegel, P. M. W. Gill, B. G. Johnson, M. A. Robb, R. A. Cheeseman, T. A. Keith, G. A. Petersson, J. A. Montgomery, K. Raghavachari, M. A. Al-Laham, V. G. Zakrzewski, J. V. Ortiz, J. S. Foresman, J. Cioslowski, B. B. Stefanov, A. Nanayakkara, M. Challacombe, C. Y. Peng, P. Y. Ayala, W. Chen, M. W. Wong, J. L. Andres, E. S. Replogle, R. Gomperts, R. L. Martin, D. J. Fox, J. S. Binkley, D. J. Defrees, J. Baker, J. J. P. Stewart, M. H. Gordon, C. Gonzalez, and J. A. Pople, Gaussian Inc., Pittsburgh, PA, 1995.

[18] R. W. G. Wyckoff, in *Crystal Structures* (Wiley, New York, 1963), Vol. 1, p.312.
[19] K. Ohkubo, Y. Igari, S. Tomada, and I. Kusunoki, Surf. Sci. **260**, 44 (1992).
[20] Y. K. Sun, D. J. Bonser, and T. Engel, Phys. Rev. B **43**, 14 309 (1991); J. Vac. Sci. Technol. A **10**, 2314 (1992).
[21] K. E. Johnson and T. Engel, Phys. Rev. Lett. **69**, 339 (1992).
[22] K. Tsukui, K. Endo, R. Hasunuma, O. Hirabayashi, N. Yagi, H. Aihara, T. Osaka, and I. Ohdomari, Surf. Sci. **328**, L553 (1995), and references therein.
[23] T. Hoshino, K. Kumamoto, K. Kokubun, T. Ishimaru, and I. Ohdomari, Phys. Rev. B **51**, 14 594 (1995); T. Hoshino, K. Kokubun, H. Fujiwara, K. Kumamoto, T. Ishimaru, and I. Ohdomari, Phys. Rev. Lett. **75**, 2372 (1995); K. Kumamoto, T. Hoshino, K. Kokubun, T. Ishimaru, and I. Ohdomari, Phys. Rev. B **53**, 12 907 (1996).
[24] T. Hoshino, K. Kokubun, K. Kumamoto, T. Ishimaru, and I. Ohdomari, Jpn. J. Appl. Phys., Part 1 **34**, 3346 (1995); K. Kumamoto, T. Hoshino, K. Kokubun, T. Ishimaru, and I. Ohdomari, Phys. Rev. B **52**, 10 784 (1995); T. Hoshino, T. Ishimaru, K. Kumamoto, H. Kawada, and I. Ohdomari, Appl. Surf. Sci. **107**, 53 (1996).
[25] K. Edamoto, Y. Kubota, H. Kobayashi, M. Onchi, and M. Nishijima, J. Chem. Phys. **83**, 428 (1985).
[26] CODATA recommended key values for thermodynamics, J. Chem. Thermodyn. **10**, 903 (1978).
[27] T. Hattori, Oyo Butsuri **64**, 1085 (1995).
[28] For example, S. Oikawa and M. Tsuda, J. Am. Chem. Soc. **107**, 1940 (1985).